



Title	Decarboxylative Functionalization of Carboxylic Acids with Easily Oxidizable, Unstable, and Difficult Substituents Under Visible Light Irradiation
Author(s)	Tamaki, Sota; Kusamoto, Tetsuro; Tsurugi, Hayato
Citation	ChemCatChem. 2025, p. e202402106
Version Type	VoR
URL	<a href="https://hdl.handle.net/11094/100964">https://hdl.handle.net/11094/100964</a>
rights	This article is licensed under a Creative Commons Attribution-NonCommercial-NoDerivatives 4.0 International License.
Note	

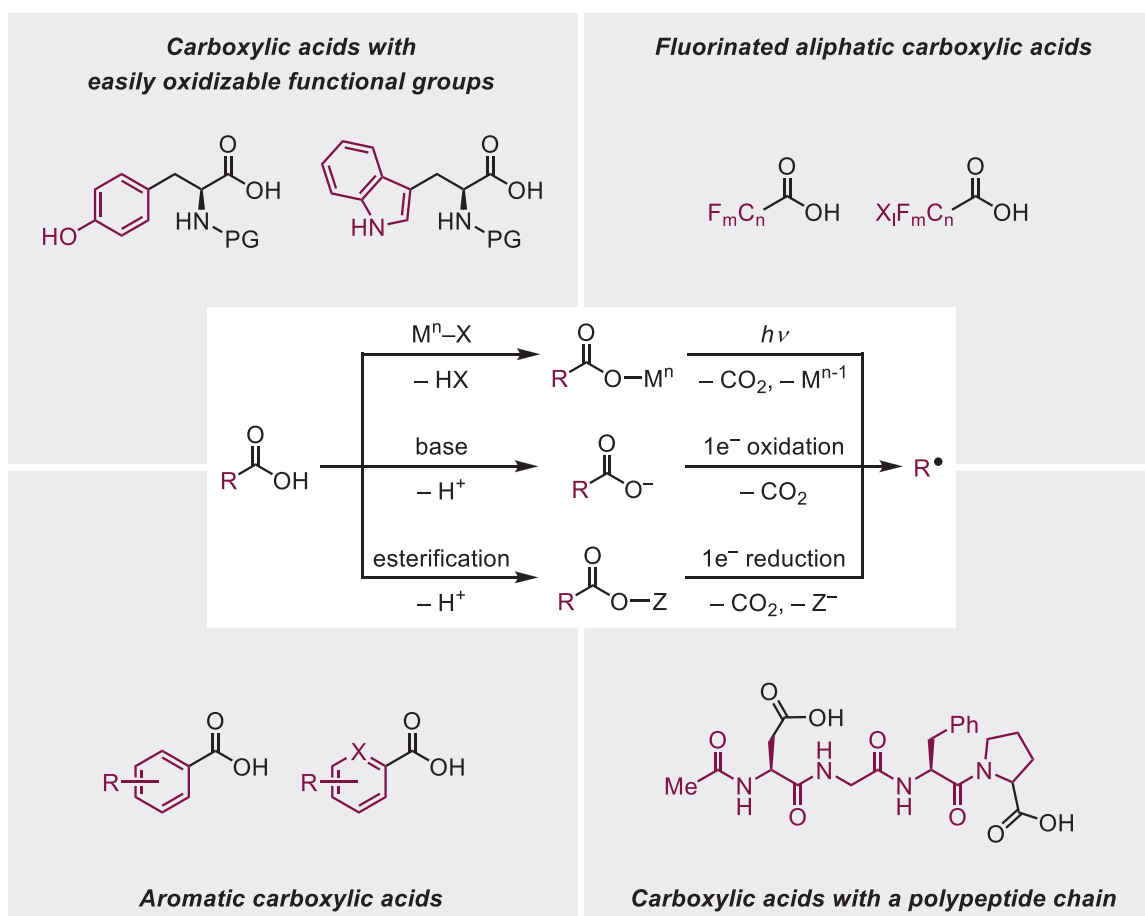
*The University of Osaka Institutional Knowledge Archive : OUKA*

<https://ir.library.osaka-u.ac.jp/>

The University of Osaka

# Decarboxylative Functionalization of Carboxylic Acids with Easily Oxidizable, Unstable, and Difficult Substituents Under Visible Light Irradiation

Sota Tamaki,<sup>[a]</sup> Tetsuro Kusamoto,<sup>[a]</sup> and Hayato Tsurugi\*<sup>[b, c]</sup>



Decarboxylative functionalization of carboxylic acids via carboxyl radical generation is an important strategy in organic synthesis. Carboxylic acids, widely found in nature as amino acids, peptides, fatty acids, and sugar acids, have the high abundance, accessibility, and stability. Decarboxylation of simple carboxylic acids such as acetic acid and fluoroalkyl carboxylic acids leads to the formation of synthetically useful methyl and fluoroalkyl radicals. The high stability of the carboxyl group toward air and moisture as well as the high functional group tolerance of radical reactions enable the application of aliphatic carboxylic acid

functionalities in late-stage transformations during the synthesis of complicated organic molecules, such as natural products and pharmaceuticals. This review focuses on recent advancements in decarboxylative functionalization under visible light irradiation, highlighting carboxylic acids with easily oxidizable, unstable, and difficult substituents. In addition to visible-light-induced transformations, this review summarizes electrochemical and thermal reactions as complementary methods for decarboxylative transformations.

## 1. Introduction

The utilization of organic radicals derived from carboxylic acids is important because of the high abundance, accessibility, and stability of carboxylic acids that are found in nature as amino acids, peptides, fatty acids, sugar acids, and so on. In addition, due to the limited availability of fossil fuels and the negative environmental impact of their consumption, changing carbon resources from fossil fuels to renewable resources has become highly desirable in recent years. In this regard, the development of transition metal catalysts for converting sustainable organic resources such as carboxylic acids into value-added chemicals via decarboxylation is highly demanded in both academia and industry.<sup>[1]</sup>

Various decarboxylative transformations of aliphatic carboxylic acids have undergone significant development due to the faster decarboxylation process of aliphatic carboxyl radicals ( $k \sim 10^9 \text{ s}^{-1}$ ) compared with that of aromatic carboxyl radicals ( $k \sim 10^6 \text{ s}^{-1}$ ).<sup>[2]</sup> Decarboxylation of simple carboxylic acids such as acetic acid and fluoroalkyl carboxylic acids via carboxyl radical generation produces less stable but synthetically useful methyl and fluoroalkyl radicals. The high stability of the carboxyl group toward air and moisture as well as the high functional group tolerance of radical reactions enable the application of aliphatic carboxylic acid functionalities in late-stage transformations during the synthesis of complicated organic molecules, such as natural products and pharmaceuticals. In this review, based on the synthetic utilities of carboxylic acids via decarboxylation, we overview the applications of carboxylic acids and their

derivatives for radical generation and radical-mediated organic transformations. In addition to decarboxylation via carboxyl radicals, a nonradical mechanism is reported for noble transition metal carboxylates, giving arylmetal species; details on the arylmetal formation from metal carboxylates are summarized in the relevant review articles.<sup>[3]</sup>

Organic radicals are formed from aliphatic carboxylic acids using metal carboxylates, carboxylic acids, or carboxylic acid derivatives, in which carboxyl radicals are generated in the reaction mixture for the following decarboxylation step, as summarized in Scheme 1. Due to the acidic nature of carboxylic acids, metal carboxylates are easily formed upon reaction with basic metal salts or organic/inorganic bases. Successive photo-irradiation results in homolysis of the metal–carboxylate bond to produce carboxyl radicals when the metal center has a high oxidation state and possesses redox-active properties (path a-i),<sup>[4]</sup> while oxidation of silver carboxylates with  $X_2$  ( $X = \text{Cl}, \text{Br}, \text{I}$ ) results in the formation of carboxyl radicals via acyl hypohalites (path a-ii).<sup>[5]</sup> Anodic or photocatalytic oxidation of the carboxylate salts of alkaline metals gives carboxyl radicals (path b).<sup>[1b,d]</sup> Upon reaction with hydrogen atom transfer reagents, carboxyl radicals are directly generated from carboxylic acids; however, the bond dissociation energy for the O–H bond is relatively high ( $112 \pm 3 \text{ kcal mol}^{-1}$ ),<sup>[6]</sup> and this method is rarely been explored (path c).<sup>[7]</sup> In contrast, esterification of carboxylic acids is widely used to generate synthetically useful reactive esters for the formation of carboxyl radicals. Early examples are the Barton esters using pyridine as an esterification agent of carboxylic acids, and post-treatment with organic radicals affords carboxyl radicals along with pyridyl thioethers (path d).<sup>[8]</sup> When *N*-hydroxyphthalimide (NHPI) derivatives or iodoarene diacetates are used for the esterification agents, redox-active esters are formed in the reaction mixture, and subsequent single electron reduction by external reagents such as metal reductants, photocatalysts, or via electrolysis gives carboxyl radicals together with phthalimide or iodoarene (path e).<sup>[9]</sup> In addition, by derivatizing to oxime esters, triplet energy transfer from excited photocatalysts induces N–O bond homolysis to afford carboxyl radicals (path f).<sup>[10]</sup> Among the various methods, homolysis of the metal carboxylates under photo-irradiation, combined with suitable metal salts and oxidants, is the most promising strategy for catalytic processes as this approach avoids the formation of stoichiometric amounts of byprod-

[a] S. Tamaki, Prof. Dr. T. Kusamoto  
Department of Chemistry, Graduate School of Engineering Science, Osaka University, Toyonaka, Osaka, Japan

[b] Prof. Dr. H. Tsurugi  
Department of Applied Chemistry, Graduate School of Engineering, Osaka University, Suita, Osaka, Japan  
E-mail: [tsurugi@chem.eng.osaka-u.ac.jp](mailto:tsurugi@chem.eng.osaka-u.ac.jp)

[c] Prof. Dr. H. Tsurugi  
Innovative Catalysis Science Division, Institute for Open and Transdisciplinary Research Initiatives (IOTS-OTRI), Osaka University, Suita, Osaka, Japan

© 2025 The Author(s). ChemCatChem published by Wiley-VCH GmbH. This is an open access article under the terms of the [Creative Commons Attribution-NonCommercial-NoDerivs](#) License, which permits use and distribution in any medium, provided the original work is properly cited, the use is non-commercial and no modifications or adaptations are made.

ucts associated with the additional esterification agents in paths d–f.

Various methods for generating alkyl radicals via decarboxylation of aliphatic carboxylic acids have been developed to date using many types of carboxylic acids available from natural and non-natural resources. However, decarboxylative transformations of carboxylic acids with some specific functional groups remain challenging; such carboxylic acids are roughly categorized into the following four types: (1) carboxylic acids with easily oxidizable functional groups,<sup>[11–22]</sup> (2) fluorinated aliphatic carboxylic acids,<sup>[23–36]</sup> (3) aromatic carboxylic acids,<sup>[37–41]</sup> and (4) carboxylic acids with a polypeptide chain.<sup>[42–44]</sup> Here, we provide an overview of the synthetic applications of such carboxylic acids, and the catalytic systems and reaction mechanisms used to overcome the difficulties in generating the carboxyl radicals are described according to the category.

## 2. Carboxylic Acids with Easily Oxidizable Functional Groups

### 2.1. Homolysis of a Metal–Carboxylate Bond (Path a-i)

Photo-induced homolysis of a metal–carboxylate bond is advantageous in terms of the high chemo-selectivity and site-selectivity in generating carboxyl radicals with various functional

groups. Simple aliphatic polyamine-ligated iron catalysts, particularly a diethylenetriamine (L1)-ligated complex, facilitated decarboxylative Giese-type additions of a wide range of carboxylic acids with electron-deficient alkenes, giving the decarboxylative alkylated products 1 (Scheme 2a).<sup>[11]</sup> Under the reaction conditions, *N*-protected amino acids 2 and 3 containing a phenol or thioether group were applicable with benzyl acrylate to afford 1 in high yields without oxidation of the functional groups. A proposed mechanism of this reaction is shown in Scheme 2b.

In the reaction mixture, L1-coordinated iron(III) trichloride complex A is initially generated, and subsequent ligand exchange in the presence of the carboxylic acids and *N,N*-diisopropylethylamine gives iron(III) carboxylate complex B. Then, photo-induced homolysis of the iron(III)–carboxylate bond leads to the formation of iron(II) complex C and carboxyl radical D. The radical D undergoes  $\beta$ -scission to give alkyl radical E along with CO<sub>2</sub>, followed by radical addition to benzyl acrylate, producing electron-deficient radical species F whose reduction by C in the presence of a carboxylate anion produces iron(III) species B and carbanion G. Finally, protonation of G leads to the product 1.

We successfully achieved decarboxylative Giese-type reactions of carboxylic acids 5 and 6 having a phenol or indole, typical easily oxidizable functional groups, using a catalytic amount of Fe(OAc)<sub>2</sub>(OH) and benzimidazole (L2) under blue LED irradiation (Scheme 3a).<sup>[12]</sup> During the catalytic reac-



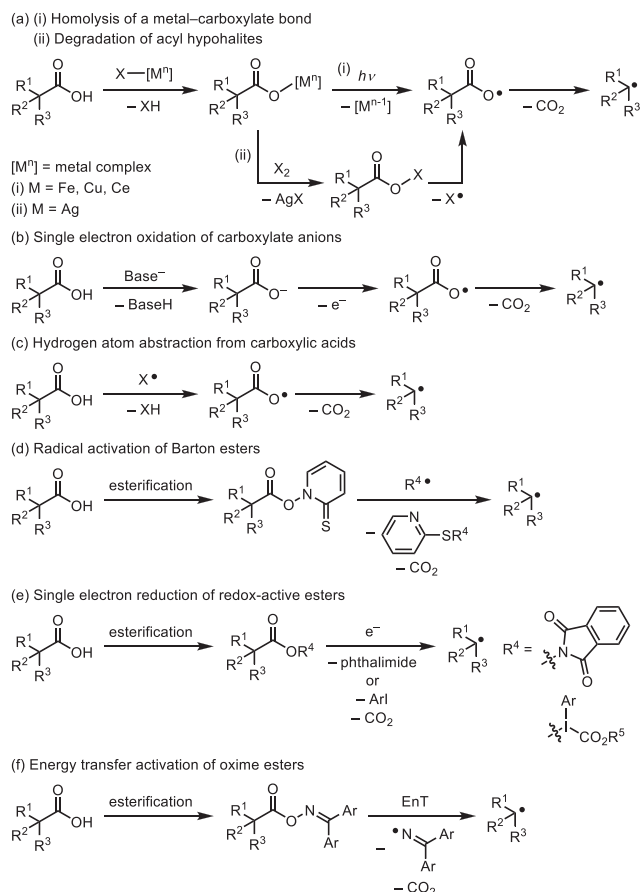
Sota Tamaki received his master's degree in 2022 under the supervision of Prof. K. Mashima at Osaka University. He is currently a Ph.D. candidate working under the guidance of Prof. T. Kusamota at Osaka University. His research focuses on decarboxylative functionalization of carboxylic acids catalyzed by metal clusters under visible light irradiation.



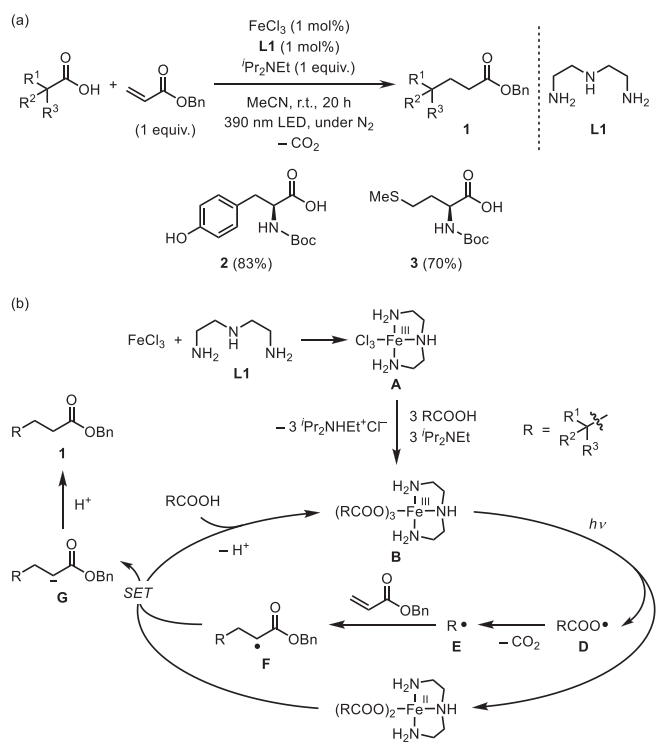
Tetsuro Kusamota received his Ph.D. in 2010 from the University of Tokyo under the supervision of Prof. Hiroshi Nishihara. After spending two and a half years at RIKEN and six years at the University of Tokyo, he was appointed as an Associate Professor at the Institute for Molecular Science in 2019. Since 2023, he has been serving as a Professor in the Department of Materials Engineering Science, Graduate School of Engineering Science, Osaka University. His research focuses on developing novel open-shell molecular systems with correlated photonic-electronic-magnetic functions.



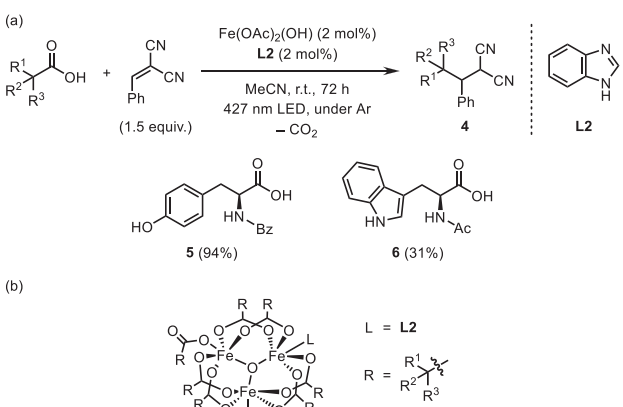
Hayato Tsurugi is working as a full professor at Department of Applied Chemistry, Graduate School of Engineering, Osaka University since April 2024. He obtained his Ph.D. degree in 2006 from Graduate School of Engineering Science, Osaka University under the supervision of Prof. K. Mashima. He mainly works on organometallic chemistry and catalysis of early transition metals and rare earth metals, photo-active multi-metallic clusters, and organosilicon chemistry utilizable as organic reductants.



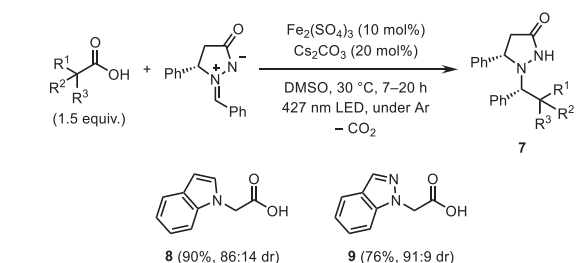
Scheme 1. Formation of alkyl radicals from aliphatic carboxylic acids.



Scheme 2. (a) Iron-catalyzed decarboxylative Giese-type addition. (b) Proposed mechanism.



Scheme 3. (a) Decarboxylative alkylation catalyzed by imidazole-coordinated iron clusters. (b) Catalytically active trinuclear iron(III) clusters H.

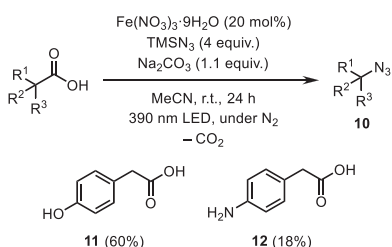


Scheme 4. Diastereoselective iron-catalyzed decarboxylative C–C bond formation.

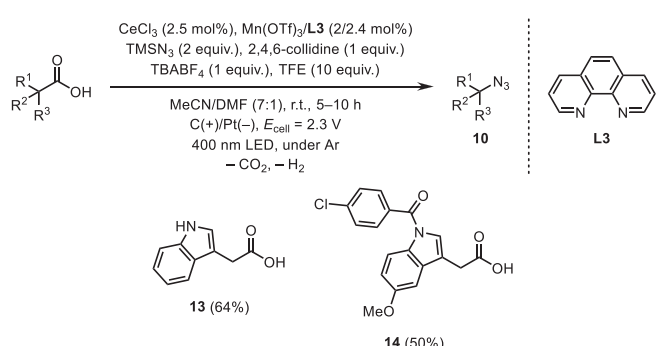
tion, L2-coordinated oxo-centered trinuclear iron(III) clusters  $\text{Fe}_3\text{O}(\text{OCOR})_7(\text{L2})_n$  ( $n = 1 - 3$ , H) are generated as the photo-responsive species for the carboxyl radical generation, which was determined by the ESI-MS analyses of the reaction mixture. In this photo-reduction step, an  $\eta^1$ -carboxylate ligand on the iron(III) center is assumed to be more reactive compared with bridging carboxylates (Scheme 3b). Coordination of L2 to the iron(III) cluster increased the absorption of visible light, resulting in enhancing the photocatalytic performance compared with the ligand-free conditions. The iron(III) cluster catalysts were also applicable for phenol-containing alkenes.

Diastereoselective iron-catalyzed decarboxylative C–C bond formation was reported using chiral azomethine imines as the radical acceptors under visible light to afford the corresponding cyclic hydrazine derivatives 7 (Scheme 4).<sup>[13]</sup> Steric bulkiness next to the imine nitrogen atom affected the diastereoselectivity in the radical addition step. N-Carboxymethyl indole 8 and indazole 9 gave the addition products 7 in excellent yields in a highly diastereoselective manner without any specific supporting ligands.

Iron(III) nitrate catalyzed the decarboxylative azidation of carboxylic acids in the presence of  $\text{TMN}_3$  and  $\text{Na}_2\text{CO}_3$  under photo-irradiation (Scheme 5).<sup>[14]</sup> In this system, re-oxidation step is required for the catalytic conversion;  $\text{NO}_x$  derived from iron(III) nitrate serve as oxidants, thereby excluding additional oxidants and demonstrating broad functional group tolerance. In the C–N bond-forming step, in situ-generated iron(III) azide reacts with



Scheme 5. Decarboxylative azidation catalyzed by iron(III) nitrate.



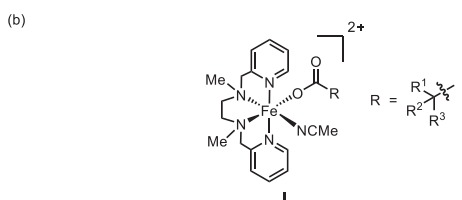
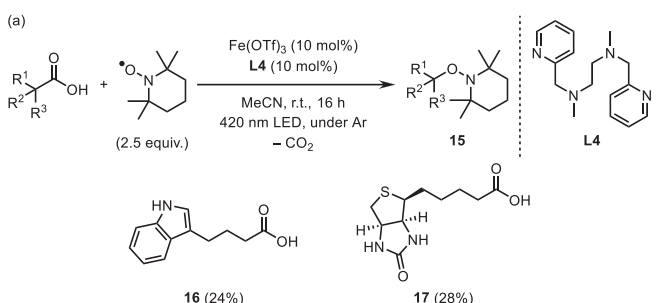
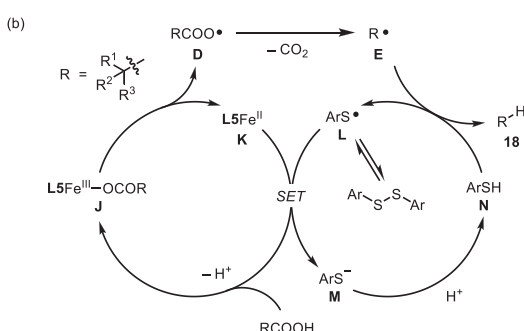
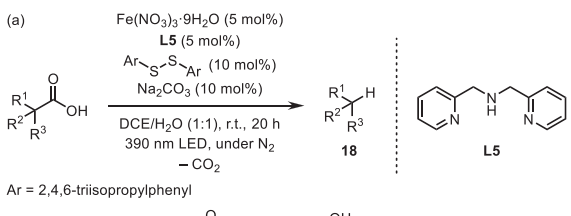
Scheme 6. Electrochemical decarboxylative azidation.

alkyl radicals derived from carboxylic acids to produce azidation products **10** along with iron(II) species. Carboxylic acids **11** and **12** having non-protected phenol and aniline moieties are both applicable.

An electrochemical decarboxylative azidation of carboxylic acids was developed using a cerium-manganese dual catalytic system (Scheme 6).<sup>[15]</sup> In the reaction, cerium(IV) carboxylate species are generated for the photo-induced carboxyl radical generation, while in situ-generated manganese(III) azide serves as the azide donor for alkyl radicals under anodic oxidation conditions to afford organic azides **10**. Due to the low anodic potential to form the cerium(IV) and manganese(III) species, oxidation-sensitive *N*-heterocyclic acetic acid derivatives **13** and **14** are both applicable under the reaction conditions.

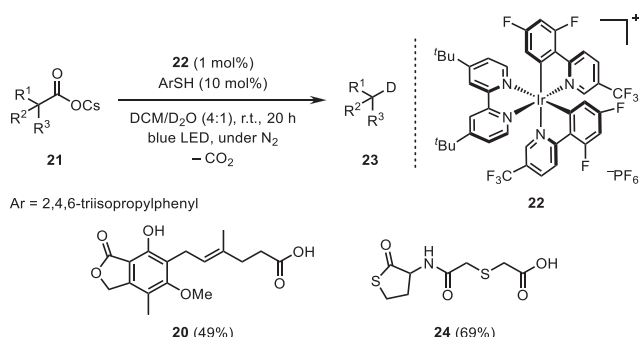
A visible light-driven iron-catalyzed decarboxylative oxygenation of carboxylic acids was achieved using TEMPO derivatives, which served as oxygenation reagents for alkyl radicals, oxidants for regenerating the iron(III) species, and bases for deprotonating carboxylic acids during a disproportionation reaction (Scheme 7a).<sup>[16]</sup> Control experiments suggest that **L4**-ligated iron(III) carboxylate complex **I**,  $[(\mathbf{L4})\text{Fe}(\text{OCOR})(\text{NCMe})]^{2+}$ , is the photo-responsive species under the catalytic reaction conditions (Scheme 7b). This reaction exhibited broad substrate scope and high functional group tolerance, including oxidation-sensitive substrates such as **16** and **17** with an indole or thioether group, though the yields of the corresponding decarboxylative oxygenated products **15** were low in both cases.

A cooperative iron/thiol catalyst system realized chemoselective decarboxylative protonation of carboxylic acids to give one carbon-shortened hydrocarbons under photo-irradiation (Scheme 8a).<sup>[17]</sup> Electron-rich arene-substituted carboxylic acids **19** and **20** afforded the corresponding products **18** in high yields.

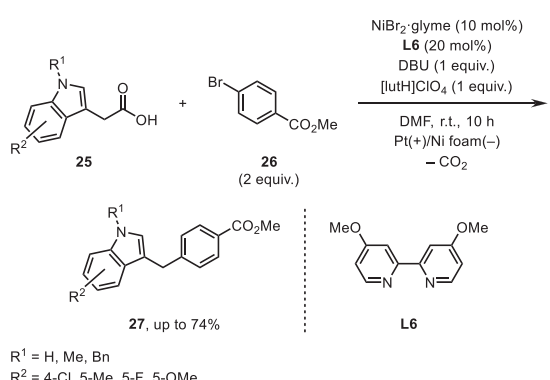
Scheme 7. (a) Iron-catalyzed decarboxylative oxygenation. (b) Proposed structure of mononuclear catalytically active species **I**.

Scheme 8. (a) Decarboxylative protonation by the iron/thiol system. (b) Plausible mechanism.

A plausible mechanism of the iron/thiol-catalyzed decarboxylative protonation is shown in Scheme 8b. First, in situ-generated **L5**-coordinated iron(III) carboxylate complex **J** undergoes homolysis of the iron(III)–carboxylate bond under photo-irradiation to give carboxyl radical **D** and photo-reduced iron(II) complex **K**. In situ-generated thiol radical **L** derived from bis(2,4,6-triisopropylphenyl) disulfide oxidizes **K** to generate iron(III) complex **J** in the presence of a carboxylic acid and thiolate anion **M**. Protonation of **M** affords thiol **N**, which serves as a hydrogen atom donor for alkyl radical **E**, affording the decarboxylative protonated product **18**.



**Scheme 9.** Decarboxylative deuteration of cesium carboxylates.

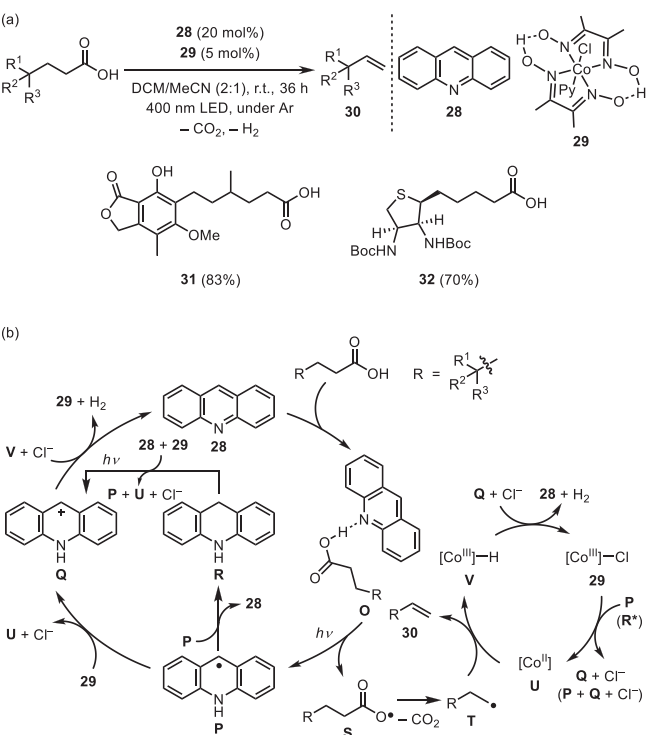


**Scheme 10.** Nickel-catalyzed decarboxylative cross-coupling substituted indole-3-acetic acids by convergent paired electrolysis.

## 2.2. Single-Electron Oxidation of Carboxylate Anions (Path b)

Alkali metal carboxylates ( $\text{RCO}_2\text{M}$ ,  $\text{M} = \text{Na, K, Cs}$ ), formed by treating carboxylic acids with  $\text{MOH}$ , possess lower redox potentials compared with other carboxylate metal salts.<sup>[18]</sup> Cesium carboxylates **21** are typical examples of facial oxidation, leading to the formation of carboxyl radicals; easily oxidizable functionalities on the carboxylate anion facilitate the one-electron oxidation. Notably, cesium salts derived from oxidation-sensitive bio-active carboxylic acids **20** and **24** were transformed to the corresponding decarboxylative deuterated products **23** under blue LED light irradiation in the presence of iridium photoredox catalyst **22** and 2,4,6-triisopropylbenzenethiol in  $\text{DCM}/\text{D}_2\text{O}$  as the mixed solvent (Scheme 9).

Convergent paired electrolysis enabled a L6-coordinated nickel-catalyzed decarboxylative cross-coupling of substituted indole-3-acetic acids **25** and aryl bromide **26** in an undivided cell (Scheme 10).<sup>[19]</sup> In this process, organic radicals derived from **25** are trapped by the nickel(II) species, which is generated by oxidation addition of **26** to nickel(I) species and subsequent cathodic reduction. The anode potential is sufficient to promote one-electron oxidation of carboxylate anions generated upon reacting with DBU, and the cathode potential corresponds to the selective reduction of nickel(II) to nickel(I) rather than further reduction to nickel(0).

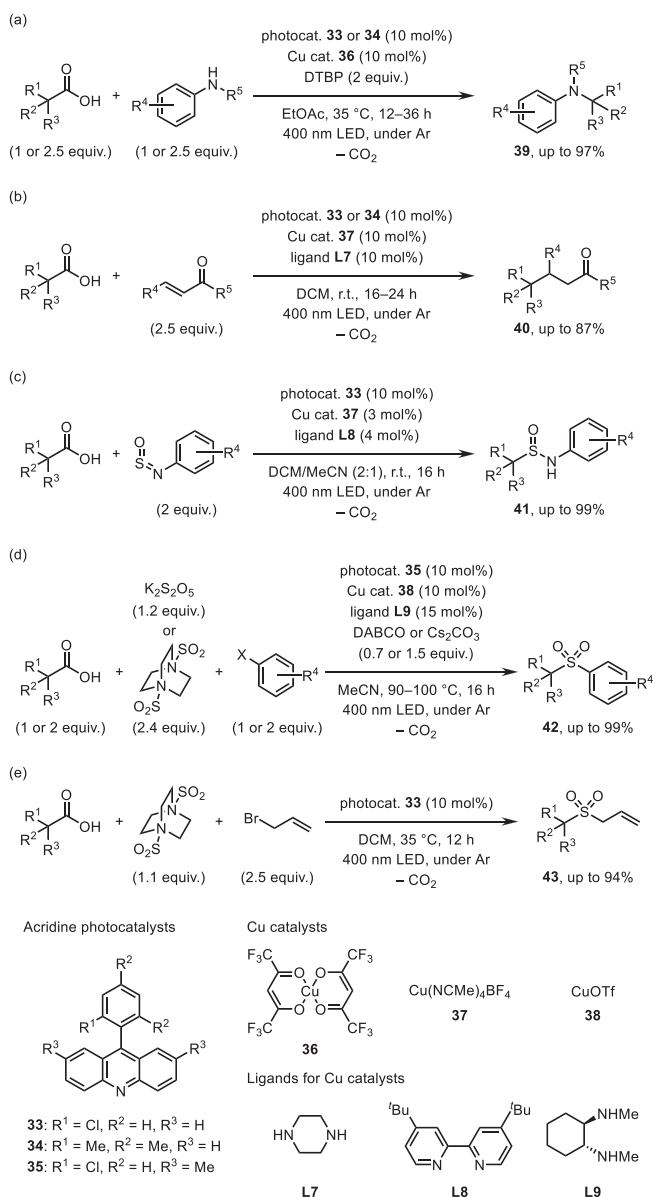


**Scheme 11.** (a) Dehydrodecarboxylation catalyzed by the acridine/cobaloxime system. (b) Proposed mechanism.

### 2.3. Hydrogen Atom Abstraction from Carboxylic Acids (Path c)

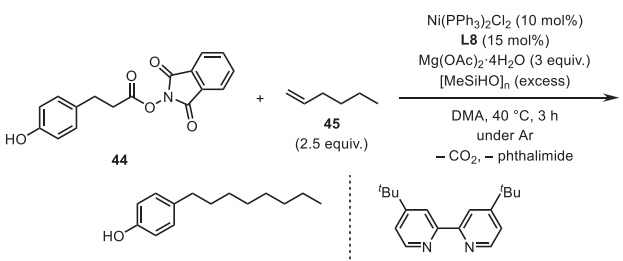
In recent years, Larionov et al. intensively studied acridine photocatalysts for decarboxylation through proton-coupled electron transfer (PCET).<sup>[7c-h]</sup> Their seminal study on a dual catalytic system using acridine (28) and cobaloxime 29 demonstrated the synthesis of various alkenes 30 via dehydrodecarboxylation of carboxylic acids (Scheme 11a).<sup>[7c]</sup> This catalytic system is effective for derivatizing bio-active carboxylic acids 31 and 32. Based on their mechanistic studies, a dual catalytic reaction mechanism is proposed as shown in Scheme 11b. Acridine (28) interacts with a carboxylic acid to give "hydrogen-bonded" complex O. By photo-induced PCET, O produces acridinyl radical P and carboxyl radical S. P is oxidized by Co<sup>III</sup> cobaloxime 29 to afford acridinyl cation Q and Co<sup>II</sup> cobaloxime U. Disproportionation of P also occurs to generate 31 and 9,10-dihydroacridine (R), the latter of which is photo-excited to form R\*, which reduces 29, forming acridinyl cation Q and cobalt(II) species U. Cobalt(II) species U mediates  $\beta$ -hydrogen abstraction from alkyl radical T, generated from S via decarboxylation, affording the desired alkenes 30 and Co<sup>III</sup> hydridocobaloxime V. Finally, V reacts with Q and chloride to regenerate 28 and 29 with the concomitant release of H<sub>2</sub>.

Acridine photocatalysts exhibit high functional group tolerance for the decarboxylation of carboxylic acids due to the formation of hydrogen-bonded complexes for the subsequent PCET process. Several decarboxylative functionalizations of various carboxylic acids containing oxidation-sensitive substituents were reported by modifying the acridine photocatalysts with

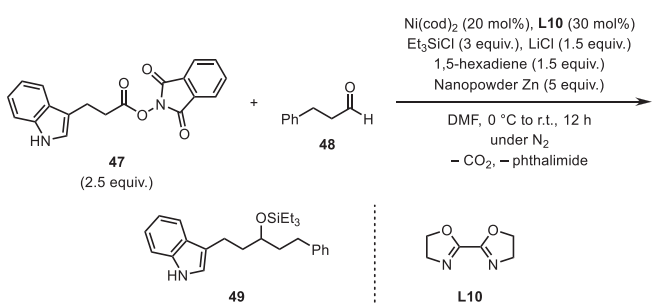


**Scheme 12.** (a) Decarboxylative *N*-alkylation. (b) Decarboxylative conjugate addition. (c) Decarboxylative sulfonamidation. (d) Decarboxylative cross-coupling. (e) Decarboxylative alkylsulfonylation.

suitable transition metal co-catalysts (Scheme 12).<sup>[7d–f]</sup> A dual catalytic system using acridine photocatalysts 33 or 34 and copper complex 36 enabled the use of carboxylic acids as alkyl sources for primary and secondary anilines to afford *N*-alkylated secondary and tertiary anilines 39 (Scheme 12a).<sup>[7d]</sup> The combination of 33 or 34 and an L7-ligated copper complex promoted a decarboxylative conjugate addition to enones, producing decarboxylative alkylated products 40 (Scheme 12b).<sup>[7e]</sup> Acridine photocatalyst 33 and an L8-ligated copper complex catalyzed decarboxylative C–S bond formation to give sulfonamides 41 using sulfinylamines as the coupling partners (Scheme 12c).<sup>[7f]</sup> A three-component decarboxylative cross-coupling reaction was reported using acridine photocatalyst 35 and an L9-ligated copper complex (Scheme 12d),<sup>[7g]</sup> in which carboxylic acids were coupled with SO<sub>2</sub> and aryl halides to form aromatic sulfones 42.



**Scheme 13.** Decarboxylative alkylation of NHPI ester 44.



**Scheme 14.** Nickel-catalyzed reductive coupling of NHPI ester 47.

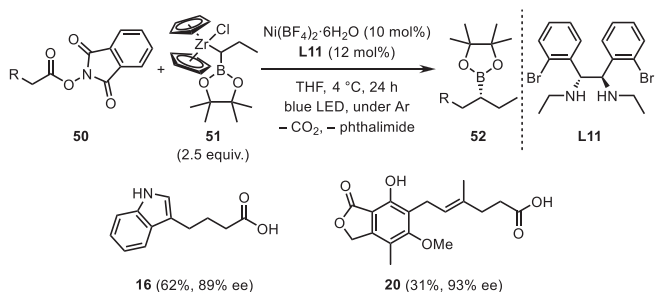
Without transition metal salts, a similar three-component coupling reaction was achieved using acridine photocatalyst 33 to give allylsulfones 43 (Scheme 12e).<sup>[7h]</sup>

#### 2.4. Single-Electron Reduction of Redox-Active Esters (Path e)

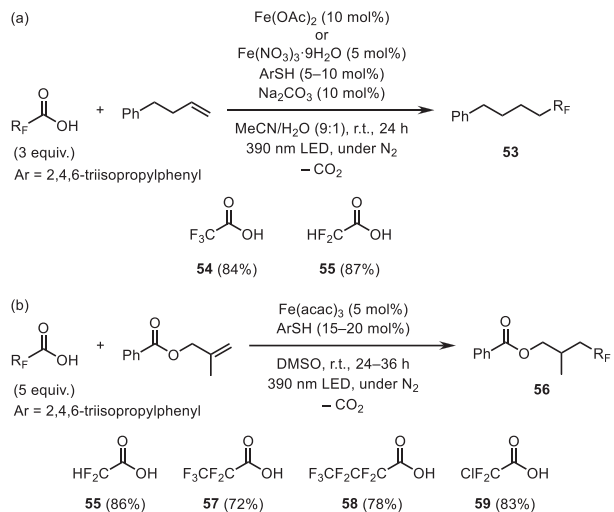
Upon one-electron reduction, NHPI esters generate the corresponding alkyl radicals along with phthalimide and CO<sub>2</sub> through decarboxylation without the degradation of oxidation-sensitive functionalities. When Ni(PPh<sub>3</sub>)<sub>2</sub>Cl<sub>2</sub> and L8 were used as the catalyst in the presence of Mg(OAc)<sub>2</sub> and an excess amount of [MeSiHO]<sub>n</sub>, decarboxylative alkylation of NHPI ester 44 having a phenol group with unactivated alkene 45 proceeded to give the product 46 in 53% yield (Scheme 13).<sup>[20]</sup>

Nickel species having L10 catalyzed a reductive coupling of NHPI ester 47 containing an indole functionality with 3-phenylpropionaldehyde (48) using zinc metal as a reductant (Scheme 14).<sup>[21]</sup> During the catalytic reaction, an in situ-generated ( $\eta^2$ -aldehyde)nickel(0) complex reacts with triethylsilyl chloride to afford a nickel(II) silyloxyalkyl complex. This nickel(II) species traps an alkyl radical generated by the reduction of 47, and subsequent reductive elimination ultimately produces silyl-protected secondary alcohol 49.

A nickel and L11 catalyst enabled an asymmetric decarboxylative C–C cross-coupling reaction between primary aliphatic acid NHPI esters 50 and a *gem*-borazirconocene alkane 51, providing practical access to a broad range of valuable chiral alkylboron products 52 having an oxidation-sensitive primary alkyl chain (16 and 20) (Scheme 15).<sup>[22]</sup> In this reaction, NHPI esters 50 are reduced by in situ-generated zirconium(III) species via homolysis of the zirconium(IV)–carbon bond in 51 under blue LED irradiation.



Scheme 15. Asymmetric decarboxylative C–C bond formation.



Scheme 16. Iron-catalyzed hydrofluoroalkylation of alkenes. (a) West's report. (b) Xia's report.

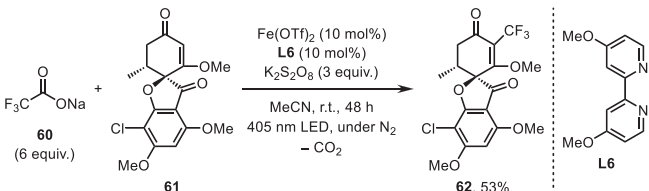
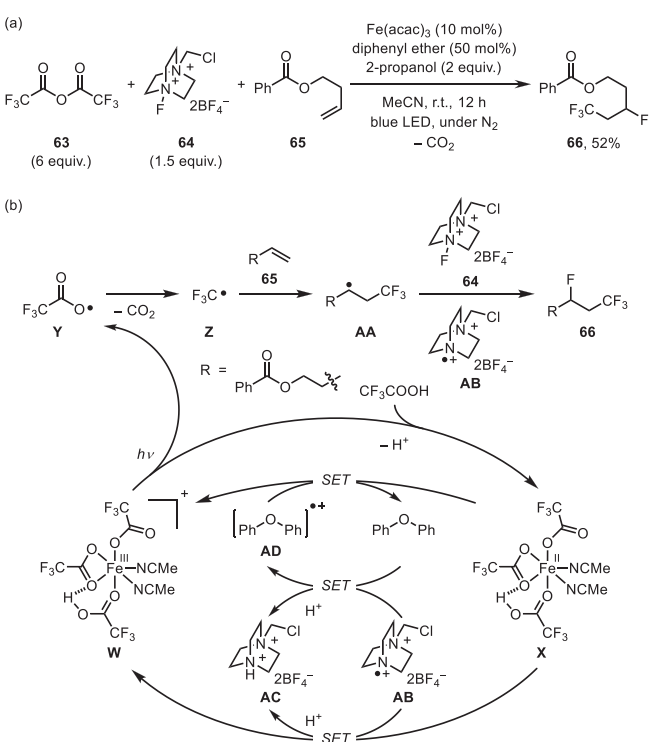
### 3. Fluorinated Aliphatic Carboxylic Acids

#### 3.1. Homolysis of a Metal–Carboxylate Bond (Path a-i)

West et al. and Xia et al. independently reported iron-catalyzed hydrofluoroalkylation of alkenes with fluorinated aliphatic carboxylic acids **54**, **55**, and **57** – **59** via decarboxylation under purple LED irradiation, affording **53** and **56** (Scheme 16).<sup>[23,24]</sup> Simple iron salts served as catalysts for decarboxylation without any specific supporting ligands, generating fluoroalkyl radicals. A bulky thiophenol was used as a co-catalyst to provide a hydrogen atom after radical addition to non-activated alkenes, generating a thiophenoxy radical that oxidized photo-reduced iron(II) species to regenerate iron(III) carboxylates.

Taking advantage of the ability to generate a trifluoromethyl radical via decarboxylation from trifluoromethyl acetate **60** under mild conditions, trifluoromethylation of multi-functional alkene **61** was investigated using an Fe/L6 catalyst and a co-oxidant  $K_2S_2O_8$  (Scheme 17).<sup>[25]</sup> In this catalytic reaction, due to the poor solubility of the strong oxidant  $K_2S_2O_8$  in MeCN, trifluoromethylation of the less-robust substrate **61** afforded trifluoromethylated alkene **62** after radical addition and oxidation of the radical center.

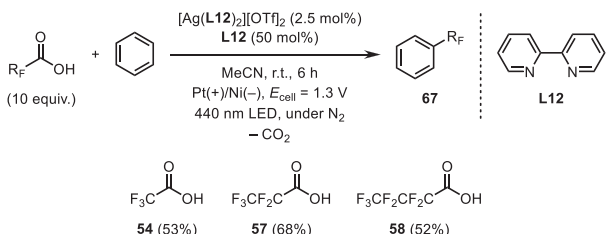
Fluoro-polyfluoroalkylation of nonactivated alkenes was achieved using  $Fe(acac)_3$ , diphenylether, and 2-propanol.<sup>[26]</sup> Tri-

Scheme 17. Trifluoromethylation of less-robust multi-functional alkene **61**.

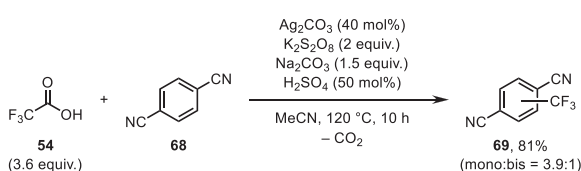
Scheme 18. (a) Fluoro-polyfluoroalkylation of nonactivated alkenes. (b) Proposed mechanism.

fluoroacetic anhydride (**63**) was used as a trifluoromethyl radical source combined with Selectfluor (**64**) and alkene **65**, giving the desired fluorotrifluoromethylated product **66** in a moderate yield (Scheme 18a). In this reaction, the combination of **63** as a trifluoromethylacetate source with 2-propanol affords trifluoroacetic acid via an ester exchange reaction. Mechanistic studies suggest the reaction mechanism of fluoro-polyfluoroalkylation of non-activated alkenes as shown in Scheme 18b. In situ-generated photo-active cationic iron(III) trifluoroacetate complex **W** undergoes homolysis of the iron(III)– $\eta^1$ -carboxylate bond in the presence of trifluoroacetic acid to give trifluoroacetoxy radical **Y** and iron(II) trifluoroacetate complex **X** under blue LED irradiation. Decarboxylation of **Y** affords trifluoromethyl radical **Z** followed by radical addition to non-activated alkene **65** to produce radical adduct **AA**. Direct radical fluorination between **AA** and Selectfluor (**64**) provides the desired fluorotrifluoromethylated product **66** and *N*-radical cation species **AB** from **64**. Radical cations **AB** and **AD** derived from diphenyl ether and **AB** oxidize iron(II) complex **X** to regenerate iron(III) complex **W**.

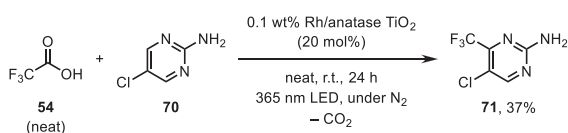
Nocera et al. utilized electrophilic silver(II) trifluoroacetate complexes to activate the silver(II)–carboxylate bond



Scheme 19. Electrochemical silver-catalyzed perfluoroalkylation of benzene.



Scheme 20. Trifluoromethylation of electron-deficient arene 68 using silver(II) species as the oxidant.

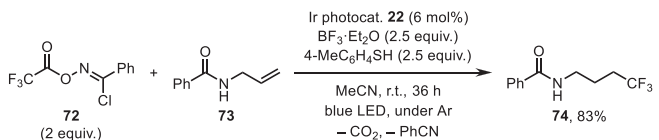
Scheme 21. C–H bond trifluoromethylation catalyzed by rhodium-decorated TiO<sub>2</sub> nanoparticles.

with visible light irradiation under electrochemical conditions (Scheme 19).<sup>[27]</sup> The generated trifluoromethyl radical reacted with a variety of arenes to form C(sp<sup>2</sup>)–CF<sub>3</sub> bonds. Carboxylic acids 57 and 58 with a longer perfluoroalkyl chain were applicable in this reaction. The generation of silver(II) species is generally difficult, but electrochemical oxidation of the silver(I) carboxylate affords the photo-active silver(II) species.

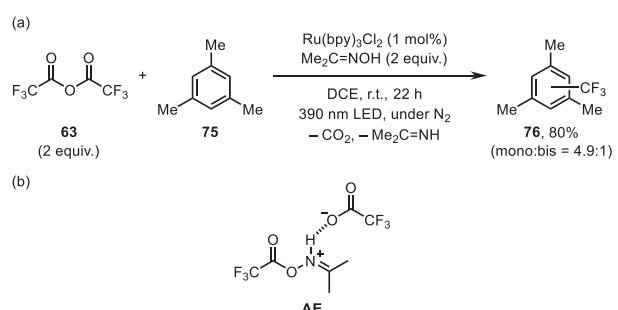
### 3.2. Single-Electron Oxidation of Carboxylate Anions (Path b)

Silver(II) species serve as an oxidant for trifluoroacetate to generate its radical along with the silver(I) species whose re-oxidation by a peroxydisulfate anion is the key step for the overall catalytic conversion.<sup>[28]</sup> A silver-catalyzed C(sp<sup>2</sup>)–H trifluoromethylation of electron-deficient arenes such as 68 was achieved using trifluoroacetic acid 54 as a trifluoromethyl radical source to produce the trifluoromethylated product 69 (Scheme 20), though harsh reaction conditions with K<sub>2</sub>S<sub>2</sub>O<sub>8</sub> as a strong oxidant and H<sub>2</sub>SO<sub>4</sub> as a strong acid were required to achieve this process.

Titanium oxide (TiO<sub>2</sub>) possesses high oxidation potential after photo-irradiation via the formation of holes in the TiO<sub>2</sub>–valence band for the direct oxidation of trifluoroacetic acid 54 to generate a trifluoromethyl radical via decarboxylation.<sup>[29]</sup> C(sp<sup>2</sup>)–H bond trifluoromethylation of arenes such as 70 proceeded to afford the trifluoromethylated arene 71 in the presence of rhodium-decorated (0.1 wt%) TiO<sub>2</sub> nanoparticles (Scheme 21). The Schottky barrier created at the interface between the rhodium and TiO<sub>2</sub> nanoparticles prevented recombination of the photo-



Scheme 22. Hydrotrifluoromethylation of alkene 73 using NHBC ester 72 as the trifluoromethyl radical source.



Scheme 23. (a) Trifluoromethylation of electron-rich arene 75 using acetoxime as the activator for trifluoroacetic anhydride 63. (b) Proposed structure of the hydrogen-bonded complex AE.

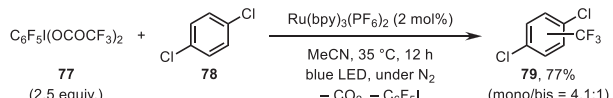
generated electron/hole pairs, thereby efficiently promoting the overall reaction.

### 3.3. Single-Electron Reduction of Redox-Active Esters (Path e)

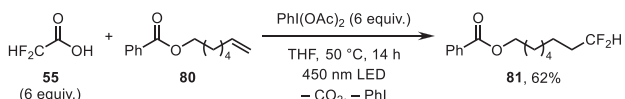
The newly developed CF<sub>3</sub>-bounded N-hydroxybenzimidoylchloride (NHBC) ester 72 was activated by the excited state of iridium photoredox catalyst 22, leading to the release of CO<sub>2</sub>, benzonitrile, and chloride anion, and generating a trifluoromethyl radical via successive N–O bond cleavage and decarboxylation (Scheme 22).<sup>[30]</sup> In addition, DFT calculations revealed that the reduction of the CF<sub>3</sub>-bearing NHBC ester 72 affords the trifluoromethyl radical and an N-centered anion species, which is in sharp contrast to the case of the well-known CF<sub>3</sub>-bearing NHPI ester, providing a trifluoroacetate anion and an N-centered radical species.

The use of acetoxime as an activator for trifluoroacetic anhydride 63 enabled the generation of a trifluoromethyl radical under photoredox catalysis, leading to the efficient C(sp<sup>2</sup>)–H trifluoromethylation of various arenes such as 75 (Scheme 23a).<sup>[31]</sup> The nucleophilic substitution reaction of 63 with acetoxime gives an acetoxime ester and trifluoroacetic acid. The acetoxime ester interacts with trifluoroacetic acid through a hydrogen bond to form a hydrogen-bonded species AE, which is easily reduced by the photo-excited ruthenium complex to give a trifluoromethyl radical and acetone imine (Scheme 23b).

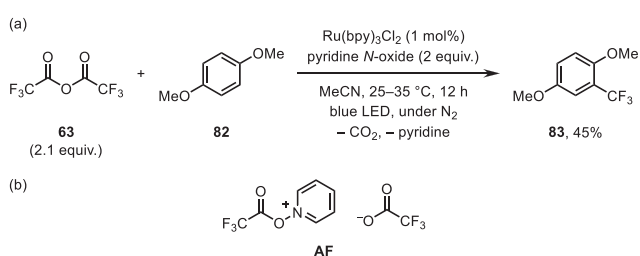
A hypervalent iodine(III) trifluoroacetate 77 provided a trifluoromethyl radical via decarboxylation using a ruthenium photoredox catalyst, resulting in the C(sp<sup>2</sup>)–H trifluoromethylation of arenes such as 78 to afford 79 (Scheme 24).<sup>[32]</sup> In this catalytic reaction, 77 is reduced by the photo-excited state of the ruthenium complex, and subsequent homolysis of I–OCOCF<sub>3</sub> bond gives a trifluoroacetoxy radical and pentafluoriodobenzene.



**Scheme 24.** Trifluoromethylation of arene **78** using the hypervalent iodine(III) trifluoroacetate **77** as the trifluoromethyl radical source.



**Scheme 25.** Hydrodifluoromethylation of alkene **80** using phenyliodine(III) diacetate as the activator.

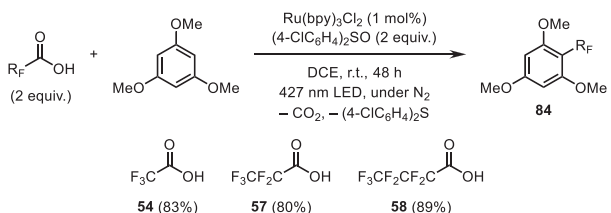


**Scheme 26.** (a) Trifluoromethylation of electron-rich arene **82** using pyridine *N*-oxide as the esterification reagent. (b) Proposed structure of trifluoroacetic anhydride adduct **AF**.

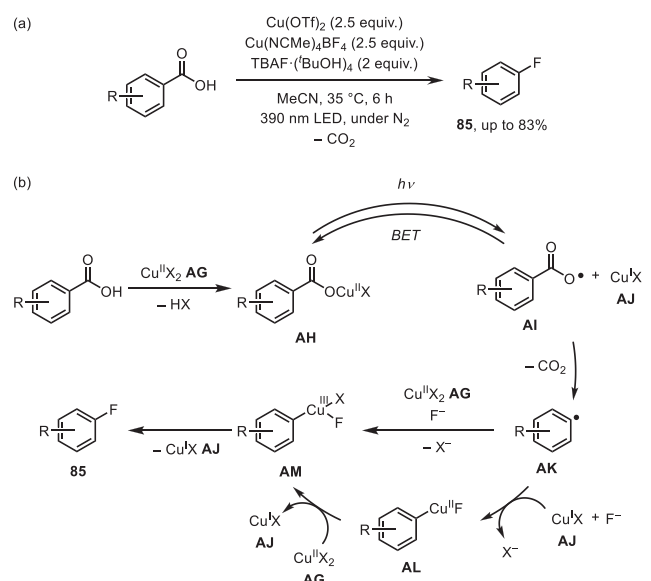
A facile method for the hydrodifluoromethylation of alkenes was reported using difluoroacetic acid (**55**) and phenyliodine(III) diacetate in tetrahydrofuran as a hydrogen donor and the solvent under visible light irradiation (Scheme 25).<sup>[33]</sup> Nonactivated alkene **80** was applicable to give the hydrodifluoromethylated product **81**. The ligand exchange of phenyliodine(III) diacetate in the presence of **55** generates phenyliodine(III) bis(difluoroacetate) whose activation by blue LED light results in decarboxylation to form a difluoromethyl radical.

A simple method for trifluoromethylating various arenes was reported via decarboxylative trifluoromethyl radical generation (Scheme 26a).<sup>[34]</sup> Pyridine *N*-oxide serves as an esterification reagent for the formation of a reducible adduct **AF** by combining with trifluoroacetic anhydride **63** (Scheme 26b). One-electron reduction of **AF** leads to the cleavage of the weak N–O bond and CO<sub>2</sub> extrusion, giving a trifluoromethyl radical with pyridine as a byproduct. Subsequent addition to electron-rich arenes such as **82** gives **83** as the final product.

Perfluoroalkyl radicals derived from **54**, **57**, and **58** were produced via visible light photoredox catalysis with the assistance of (4-ClC<sub>6</sub>H<sub>4</sub>)<sub>2</sub>SO (Scheme 27).<sup>[35]</sup> Perfluoroalkyl radicals add



**Scheme 27.** Perfluoroalkylation of 1,3,5-trimethoxybenzene with the assistance of (4-ClC<sub>6</sub>H<sub>4</sub>)<sub>2</sub>SO.



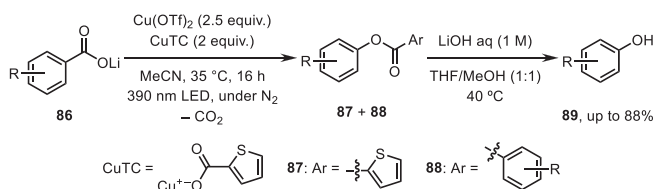
**Scheme 28.** (a) Decarboxylative fluorination using the stoichiometric amount of copper salt. (b) Proposed mechanism.

to arene substrates followed by an oxidative re-aromatization, affording the perfluoroalkylated products **84**. Although the detailed reaction mechanism is unclear, observation of thioether indicates the incorporation of the sulfoxide during the catalytic reaction.

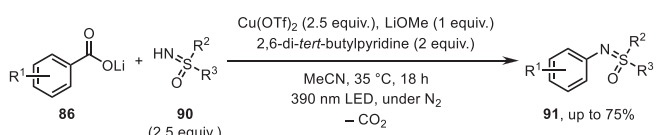
## 4. Aromatic Carboxylic Acids

### 4.1. Homolysis of a Metal–Carboxylate Bond (Path a-i)

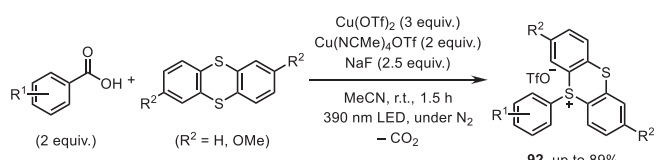
Ritter et al. extensively studied the photo-activity of copper(II) arylcarboxylate complexes for achieving the decarboxylative functionalization of aromatic carboxylic acids.<sup>[37]</sup> In 2021, they reported photo-induced homolysis of a copper(II)–carboxylate bond as a mild decarboxylative formation of high-valent aryl-copper(III) intermediates, realizing aromatic decarboxylative fluorination in the presence of a fluorine source (Scheme 28a).<sup>[37a]</sup> A proposed mechanism for the decarboxylative fluorination of aromatic carboxylic acids is shown in Scheme 28b. Coordination of an aromatic carboxylic acid to copper(II) species **AG** readily forms photo-active copper(II) carboxylate **AH**. Photo-induced homolysis of the copper(II)–carboxylate bond generates the corresponding carboxyl radical **AI** and photo-reduced copper(I) species **AJ**. Decarboxylation of **AI** produces the aryl radical **AK**, which is trapped by copper(I) species **AJ** or copper(II) species **AG**, providing arylcopper(II) fluoride **AL** or arylcopper(III) fluoride **AM**. **AL** is oxidized by copper(II) species such as **AG** to give the copper(III) species **AM** with elimination of the copper(I) species **AJ**. Finally, C(sp<sup>2</sup>)–F reductive elimination from the arylcopper(III) fluoride **AM** affords the desired aryl fluoride **85**. In this reaction, the stoichiometric in situ-generated photo-active copper(II) carboxylate **AH** is required due to the low efficiency of decarboxylation caused by back electron transfer (BET). In addition, utilization of a poor hydrogen-donating solvent such as acetonitrile



**Scheme 29.** One-pot synthesis of phenols via aromatic decarboxylative esterification.



**Scheme 30.** Transformation of lithium carboxylates **86** into *N*-arylated sulfoximines **91** using NH-sulfoximines **90** as coupling partners.



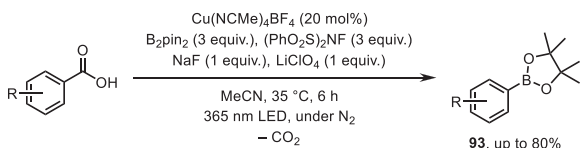
**Scheme 31.** Transformation of aromatic carboxylic acids into aryl thianthrenium salts **92**.

trile diminishes competing hydrogen atom transfer between aryl carboxyl radical **A1** and the solvent.

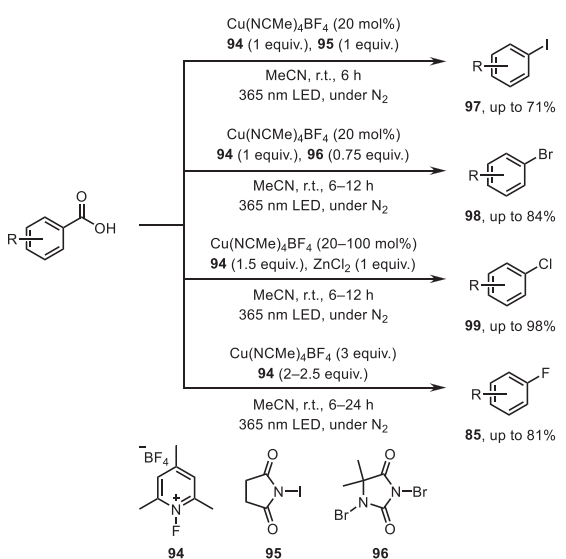
Ritter et al. also reported decarboxylative hydroxylation to synthesize phenols from benzoic acids via the formation of aryl-copper carboxylates.<sup>[37b]</sup> Photo-irradiation of a mixture of lithium carboxylate **86**, copper(II) triflate, and copper(I) thiophene-2-carboxylate (CuTC) afforded ester **87** derived from CuTC and ester **88** derived from **86**, respectively (Scheme 29). Subsequent hydrolysis resulted in the formation of phenols **89**. In this reaction, in situ-generated arylcopper(III) carboxylates having thiophene-2-carboxylate or the aryl carboxylate ligands undergo reductive elimination to afford esters **87** or **88**.

Photo-induced arylcopper carboxylate generation enabled the transformation of lithium carboxylates **86** into *N*-arylated sulfoximines **91** using NH-sulfoximines **90** as coupling partners (Scheme 30).<sup>[37c]</sup> Aryl radicals, generated from **86** via decarboxylation, are trapped by copper(I) or copper(II) species, and subsequent reaction with NH-sulfoximines forms arylcopper(III) sulfoximides. Finally, C–N reductive elimination affords the desired *N*-arylated sulfoximines **91**.

Dydo et al. reported a photo-induced copper(II)-mediated protocol for converting aromatic carboxylic acids into aryl thianthrenium salts **92** using thianthrenes as coupling partners (Scheme 31).<sup>[38]</sup> The use of poorly soluble NaF as a weak base was essential, presumably keeping a low concentration of the deprotonated carboxylic acid in solution. In contrast, the use of a stronger base such as Na<sub>2</sub>CO<sub>3</sub> or a more soluble base such as KF, which increases the concentration of the deprotonated carboxylic acid in solution, led to significant ester formation as side-products due to competitive decarboxylative self-coupling of the starting aromatic carboxylic acids.



**Scheme 32.** Copper-catalyzed decarboxylative borylation.

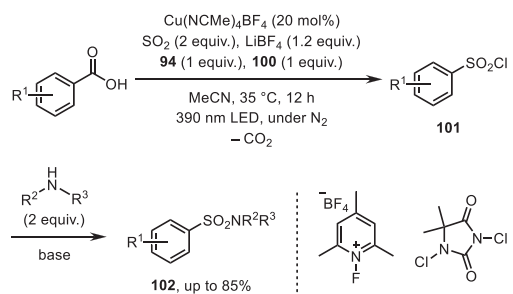


**Scheme 33.** Copper-catalyzed decarboxylative halogenation.

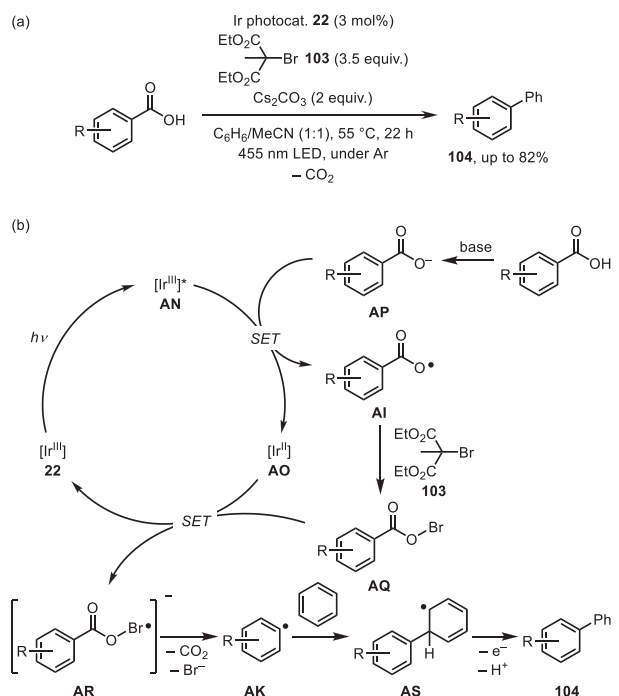
MacMillan et al. achieved copper(II)-catalyzed decarboxylative functionalization of aromatic carboxylic acids using appropriate single-electron oxidants to convert a copper(I) species into a photo-active copper(II) species.<sup>[39]</sup> Copper(II)-catalyzed decarboxylative radical generation, employing *N*-fluorobenzenesulfonimide as an oxidant, enabled decarboxylative borylation of aromatic carboxylic acids to produce aryl boronic esters **93** (Scheme 32).<sup>[39a]</sup> NaF and LiClO<sub>4</sub> serve as soluble ion sources in acetonitrile, promoting the generation of an activated lithium fluoroborate.

MacMillan et al. also reported a general strategy for the decarboxylative halogenation of aromatic carboxylic acids via photo-induced homolysis of copper(II)–carboxylate bonds (Scheme 33).<sup>[39b]</sup> In these reactions, 1-fluoro-2,4,6-trimethylpyridinium tetrafluoroborate (**94**) acts as an oxidant and fluorine source, *N*-iodosuccinimide (**95**) as an iodine source, 1, 3-dibromo-5,5-dimethylhydantoin (**96**) as a bromine source, and ZnCl<sub>2</sub> as a chlorine source. Compounds **95** and **96** serve as radical halogenation reagents for in situ-generated aryl radicals to afford the iodo- and bromodecarboxylated products **97** and **98**. In contrast, when using ZnCl<sub>2</sub> or **94** as a halogenation reagent, aryl radicals are initially trapped by copper(I) or copper(II) species, and subsequent reaction with the reagent gives the corresponding arylcopper(III) halides. These copper(II) intermediates undergo C–Cl or C–F reductive elimination to afford the chloro- and fluorodecarboxylated products **99** and **85**.

Photo-induced copper(II)-catalyzed aromatic decarboxylation enabled the conversion of aromatic carboxylic acids into sulfonyl chlorides **101** in the presence of SO<sub>2</sub> and a chlorine source



**Scheme 34.** One-pot synthesis of sulfonamides via aromatic decarboxylative halosulfonylation.

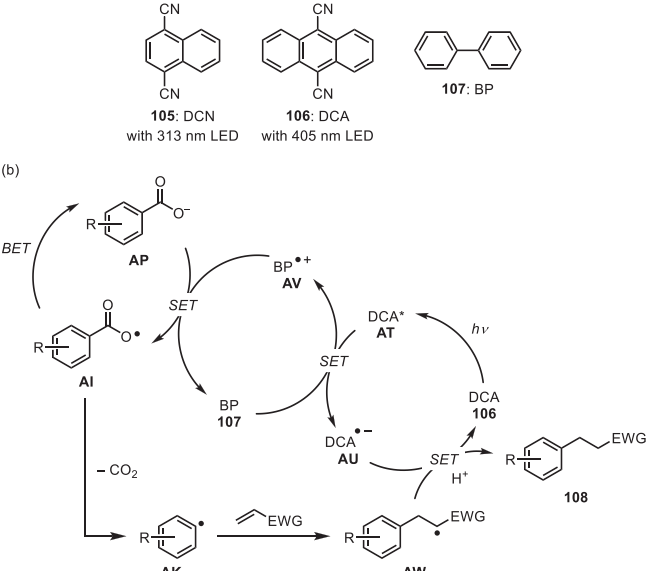
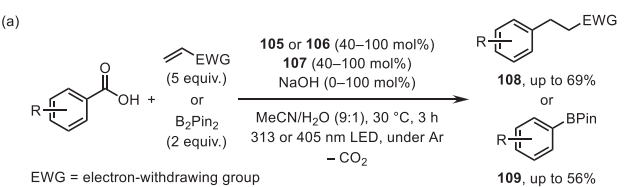


**Scheme 35.** Decarboxylative arylation through the formation of aryl hypobromites.

**100**, followed by a one-pot amination to form the corresponding sulfonamides **102** (Scheme 34).<sup>[39c]</sup>  $\text{SO}_2$  captures aryl radicals to generate aryl sulfonyl radicals for further chlorine atom abstraction, affording the sulfonyl chlorides **101**.

#### 4.2. Degradation of Acyl Hypohalites (Path a-ii)

In 2017, Glorius et al. reported the first decarboxylation of aromatic carboxylic acids to provide aryl radicals via photoredox catalysis (Scheme 35a).<sup>[40]</sup> These aryl radicals react with benzene to afford the corresponding cross-coupled biaryl products **104** according to the mechanism depicted in Scheme 35b. The aryl carboxylate anion **AP** is oxidized by the photo-excited iridium(III) complex **AN** to give the corresponding aryl carboxyl radical **AI** and the ground state of iridium(II) complex **AO**. In the presence of bromomalonate derivative **103**, **AI** is brominated to form aryl hypobromite **AQ**. Single electron reduction of **AQ** by the iridium(II) species **AO** provides radical anion **AR**, which undergoes decarboxylation to afford the aryl radical **AK**. Subsequent trapping of **AK** with benzene generates the cyclohexadienyl radical **AS**, which is then oxidized and deprotonated to afford the biaryl product **104**.

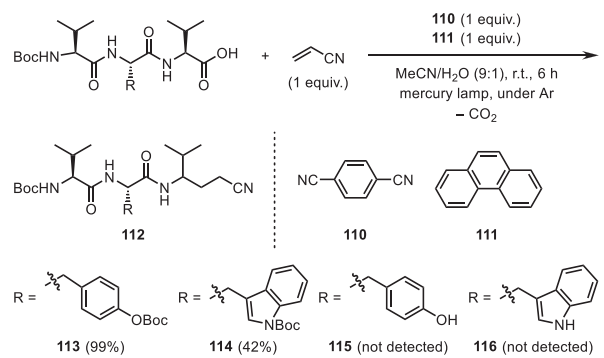


**Scheme 36.** (a) Decarboxylative alkylation and borylation using the bimolecular organophotoredox systems. (b) Proposed mechanism of decarboxylative alkylation using the DCA/BP organophotoredox system.

loyl hypobromite **AQ**. Single electron reduction of **AQ** by the iridium(II) species **AO** provides radical anion **AR**, which undergoes decarboxylation to afford the aryl radical **AK**. Subsequent trapping of **AK** with benzene generates the cyclohexadienyl radical **AS**, which is then oxidized and deprotonated to afford the biaryl product **104**.

#### 4.3. Single-Electron Oxidation of Carboxylate Anions (Path b)

Yoshimi et al. actively investigated bimolecular organophotoredox systems for decarboxylative functionalization of carboxylic acids, including aromatic carboxylic acids.<sup>[41]</sup> They reported decarboxylative Giese-type addition and borylation of aromatic carboxylic acids using electron-deficient 1,4-dicyanonaphthalene (**105**, DCN) or 9,10-dicyanoanthracene (**106**, DCA), and biphenyl (**107**, BP) as combined catalysts (Scheme 36a).<sup>[41a]</sup> Based on the control experiments, they proposed a reaction mechanism for the decarboxylative Giese-type addition of aromatic carboxylic acids catalyzed by **106** and **107** under photo-irradiation (Scheme 36b). Single-electron transfer (SET) between the photo-excited species **AT** and **107** affords the radical anion **AU** and the radical cation **AV**. Aryl carboxylate anion **AP** is then oxidized by the radical cation **AV** to generate the aryl carboxyl radical **AI**. Subsequent decarboxylation upon heating gives the aryl radical **AK**. Radical addition of **AK** to an electron-deficient alkene forms the corresponding radical adduct **AW**. Finally, reduction of



**Scheme 37.** Decarboxylative Giese-type addition of tripeptides using the bimolecular organophotoredox system.

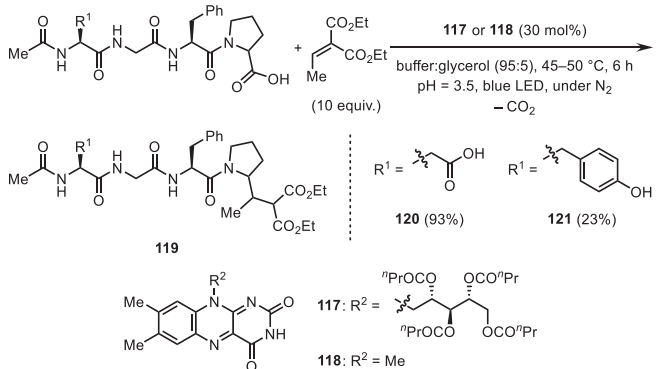
AW by the radical anion **AU** and subsequent protonation affords the decarboxylative alkylated product **108**. Photo-induced decarboxylation of aryl carboxylic acids using other typical photoredox catalysts such as an iridium complex and Fukuzumi catalyst was unsuccessful and the starting material was regenerated, probably due to the low rate of decarboxylation of **AI** and **BET** between **AI** and the reduced iridium and Fukuzumi photocatalysts. In contrast, the low efficiency of **BET** in this bimolecular organophotoredox system led to the decarboxylation of **AI**.

## 5. Carboxylic Acids with Polypeptide Chains

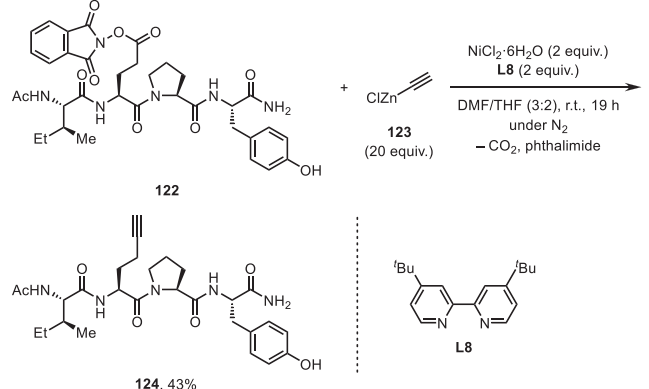
### 5.1. Single-Electron Oxidation of Carboxylate Anions (Path b)

Radical decarboxylative functionalization represents an effective strategy for late-stage peptide modification due to the high stability of the carboxyl group in the peptide toward air and moisture, as well as the high functional group tolerance of radical reactions.<sup>[41,42]</sup> Yoshimi et al. reported decarboxylative radical addition of tripeptides to electron-deficient alkenes using stoichiometric amounts of 1,4-dicyanobenzene (**110**) and phenanthrene (**111**), giving the corresponding alkylated tripeptides **112** in high to moderate yields (Scheme 37).<sup>[44d]</sup> In fact, tripeptides **113** and **114** containing Boc-protected phenol and indole moieties were compatible under the reaction conditions. The protecting group-free analogs **115** and **116** were not applicable for this reaction, however, probably due to quenching of the in situ-generated radical cation of **111** by the electron-rich arene moieties. This quenching inhibits single electron oxidation of the terminal carboxylate moiety in the tripeptides.

MacMillan et al. reported a decarboxylative Giese-type addition for bioconjugation of peptides using water-tolerant flavin photocatalysts **117** and **118** (Scheme 38).<sup>[43]</sup> Notably, tetrapeptide with two carboxyl groups **120** underwent site-selective decarboxylation at the C-terminal position because the C-terminal carboxylate is easier to oxidize, giving the corresponding C-terminal alkylated product **119**. In contrast, a peptide having a phenol group **121** afforded the decarboxylative alkylated product **119** in only 23% yield because the excited state of the photocatalyst was quenched by the phenol moiety.



**Scheme 38.** Decarboxylative Giese-type addition for bioconjugation of peptides.



**Scheme 39.** Decarboxylative C–C bond formation reactions via single electron reduction of redox-active esters installed in peptide chains.

### 5.2. Single-Electron Reduction of Redox-Active Esters (Path e)

Baran et al. reported several decarboxylative C–C bond formation reactions via single electron reduction of redox-active esters installed in peptide chains.<sup>[44]</sup> Although excess amounts of an **L8**-coordinated nickel(II) complex and ethynylzinc chloride (**123**) were required, tetrapeptide with a phenol group **122** afforded the corresponding decarboxylative alkynylated product **124** in 43% yield (Scheme 39).<sup>[44d]</sup>

## 6. Summary and Outlook

Radical decarboxylative functionalization of carboxylic acids is a powerful and versatile strategy in organic synthesis for transforming abundant natural resources into high-value chemicals. Various methods for generating alkyl radicals via decarboxylation of aliphatic carboxylic acids have been developed so far; however, decarboxylative transformations of carboxylic acids with some specific functional groups remain challenging. Among the strategies to achieve decarboxylative functionalization of carboxylic acids with some specific functional groups, photo-induced homolysis of a metal–carboxylate bond has attracted attention due to the high chemo-selectivity and site-selectivity

for generating carbon radicals having various functional groups via carboxyl radical formation and decarboxylation. Notably, this approach selectively transforms only the carboxylate bound to the metal center, making it highly effective for achieving various decarboxylative functionalization of carboxylic acids with easily oxidizable functional groups, fluorinated aliphatic carboxylic acids, and aromatic carboxylic acids. Despite the significant advancements in applying this strategy for decarboxylative transformations, its application to carboxylic acids with a polypeptide chain remains relatively unexplored. The inherent structural complexity and the presence of multiple reactive sites in the polypeptide chain make selective decarboxylation challenging. Developing more robust catalytic systems that tolerate many types of functional groups in bioactive molecules will be crucial for expanding the applicability of this methodology.

Considering the potential of this strategy, we expect that the late-stage modifications of complexed organic compounds including polypeptides will receive increasing attention in the near future.

## Acknowledgements

S.T. thanks the financial support by the JSPS Research Fellowships for Young Scientists. This work was supported by JSPS KAKENHI Grant No. JP24K01486 (Grant-in-Aid for Scientific Research(B)) to H.T.

## Conflict of Interests

The authors declare no conflict of interest.

## Data Availability Statement

Data sharing is not applicable to this article as no new data were created or analyzed in this study.

**Keywords:** Carboxylic acids · Decarboxylation · Radical · Transition-metal catalysis · Visible light

[1] a) X.-Q. Hu, Z.-K. Liu, Y.-X. Hou, Y. Gao, *iScience* **2020**, *23*, 101266; b) L. Li, Y. Yao, N. Fu, *Eur. J. Org. Chem.* **2023**, *26*, e202300166; c) J. D. Tibbetts, H. E. Askey, Q. Cao, J. D. Grayson, S. L. Hobson, G. D. Johnson, J. C. Turner-Dore, A. J. Cresswell, *Synthesis* **2023**, *55*, 3239; d) S. Mondal, S. Mandal, S. Mondal, S. P. Midya, P. Ghosh, *Chem. Commun.* **2024**, *60*, 9645; e) J.-L. Tu, Z. Shen, B. Huang, *Adv. Synth. Catal.* **2024**, *366*, 4263; f) C.-Q. Deng, J. Deng, *Green Chem.* **2025**, *27*, 275; g) C.-L. Ji, Y.-N. Lu, S. Xia, C. Zhu, C. Zhu, W. Li, J. Xie, *Angew. Chem., Int. Ed.* **2025**, *64*, e202423113; h) G.-T. Song, Y. Liu, X.-Y. Hu, S.-T. Li, J.-B. Liu, Y. Li, C.-H. Qu, *Org. Chem. Front.* **2023**, *10*, 1512; i) A. M. de Azevedo, J. G. L. de Araujo, M. S. B. do da Silva, A. S. D. dos Anjos, A. M. M. de Araújo, E. V. dos Santos, C. A. Martínez-Huitle, A. D. Gondim, L. N. Cavalcanti, *RSC Adv.* **2024**, *14*, 10755–10760; j) S. Liu, H. Liao, B. Chen, T. Guo, Z. Zhang, H. Lin, *Green Chem.* **2024**, *26*, 10456; k) Y. Xu, C. Shen, K. Dong, *J. Am. Chem. Soc.* **2025**, *147*, 6259.

[2] a) J. Chateauneuf, J. Lusztyk, K. U. Ingold, *J. Am. Chem. Soc.* **1988**, *110*, 2886; b) J. W. Hilborn, J. A. Pincock, *J. Am. Chem. Soc.* **1991**, *113*, 2683.

[3] a) N. Rodríguez, L. J. Gooßen, *Chem. Soc. Rev.* **2011**, *40*, 5030; b) J. Cornellà, I. Larrosa, *Synthesis* **2012**, *44*, 653–676; c) W. I. Dzik, P. P. Lange, L. J. Gooßen, *Chem. Sci.* **2012**, *3*, 2671; d) Y. Wei, P. Hu, M. Zhang, W. Su, *Chem. Rev.* **2017**, *117*, 8864; e) G. J. P. Perry, I. Larrosa, *Eur. J. Org. Chem.* **2017**, *3517*; f) P. J. Moon, R. J. Lundgren, *ACS Catal.* **2020**, *10*, 1742.

[4] a) Y. Abderrazak, A. Bhattacharyya, O. Reiser, *Angew. Chem., Int. Ed.* **2021**, *60*, 21100; b) F. Juliá, *ChemCatChem* **2022**, *14*, e202200916; c) S. Gavelle, M. Innocent, T. Aubineau, A. Guérinot, *Adv. Synth. Catal.* **2022**, *364*, 4189; d) X.-L. Lai, M. Chen, Y. Wang, J. Song, H.-C. Xu, *J. Am. Chem. Soc.* **2022**, *144*, 20201; e) S. Wang, T. Li, C. Gu, J. Han, C.-G. Zhao, C. Zhu, H. Tan, J. Xie, *Nat. Commun.* **2022**, *13*, 2432; f) J. Lu, Y. Yao, L. Li, N. Fu, *J. Am. Chem. Soc.* **2023**, *145*, 26774; g) N. Xiong, Y. Li, R. Zeng, *ACS Catal.* **2023**, *13*, 1678; h) M. Innocent, G. Lalande, F. Cam, T. Aubineau, A. Guérinot, *Eur. J. Org. Chem.* **2023**, *26*, e202300892; i) Y. Xu, C. Wang, C. Lv, J. Wang, Q. Zhang, J. Wang, R.-P. Shen, B. Sun, C. Jin, *New J. Chem.* **2024**, *48*, 14684; j) M. Innocent, C. Tanguy, S. Gavelle, T. Aubineau, A. Guérinot, *Chem. - Eur. J.* **2024**, *30*, e202401252; k) J. Qian, Y. Zhang, W. Zhao, P. Hu, *Chem. Commun.* **2024**, *60*, 2764; l) R. Nsouli, S. Nayak, V. Balakrishnan, J.-Y. Lin, B. K. Chi, H. G. Ford, A. V. Tran, I. A. Guzei, J. Bacsa, N. R. Armada, F. Zenov, D. J. Weix, L. K. G. Ackerman-Biegasiewicz, *J. Am. Chem. Soc.* **2024**, *146*, 29551.

[5] R. G. Johnson, R. K. Ingham, *Chem. Rev.* **1956**, *56*, 219.

[6] S. J. Blanksby, G. B. Ellison, *Acc. Chem. Res.* **2003**, *36*, 255.

[7] a) C. G. Na, D. Ravelli, E. J. Alexanian, *J. Am. Chem. Soc.* **2020**, *142*, 44; b) R. Mao, S. Bera, A. C. Turla, X. Hu, *J. Am. Chem. Soc.* **2021**, *143*, 14667; c) V. T. Nguyen, V. D. Nguyen, G. C. Haug, H. T. Dang, S. Jin, Z. Li, C. Flores-Hansen, B. S. Benavides, H. D. Arman, O. V. Larionov, *ACS Catal.* **2019**, *9*, 9485; d) V. T. Nguyen, V. D. Nguyen, G. C. Haug, N. T. H. Vuong, H. T. Dang, H. D. Arman, O. V. Larionov, *Angew. Chem., Int. Ed.* **2020**, *59*, 7921; e) H. T. Dang, G. C. Haug, V. T. Nguyen, N. T. H. Vuong, V. D. Nguyen, H. D. Arman, O. V. Larionov, *ACS Catal.* **2020**, *10*, 11448; f) H. T. Dang, A. Porey, S. Nand, R. Trevino, P. Manning-Lorino, W. B. Hughes, S. O. Fremin, W. T. Thompson, S. K. Dhakal, H. D. Arman, O. V. Larionov, *Chem. Sci.* **2023**, *14*, 13384; g) V. D. Nguyen, R. Trevino, S. G. Greco, H. D. Arman, O. V. Larionov, *ACS Catal.* **2022**, *12*, 8729; h) V. T. Nguyen, G. C. Haug, V. D. Nguyen, N. T. H. Vuong, G. B. Karki, H. D. Arman, O. V. Larionov, *Chem. Sci.* **2022**, *13*, 4170; i) X. Sui, H. T. Dang, A. Porey, R. Trevino, A. Das, S. O. Fremin, W. B. Hughes, W. T. Thompson, S. K. Dhakal, H. D. Arman, O. V. Larionov, *Chem. Sci.* **2024**, *15*, 9582; j) Q. Chen, Y. Wang, G. Luo, *Chem. Eng. J.* **2023**, *461*, 141767; k) E. Schué, D. R. L. Rickertsen, A. B. Korpusik, A. Adili, D. Seidel, B. S. Sumerlin, *2023*, *14*, 11228–11236; l) K. Bhatt, A. Adili, A. H. Tran, K. M. Elmallah, I. G., D. Seidel, *J. Am. Chem. Soc.* **2024**, *146*, 26331.

[8] M. F. Saraiwa, M. R. C. Couri, M. L. Hyaric, M. V. de Almeida, *Tetrahedron* **2009**, *65*, 3563.

[9] a) S. Murarka, *Adv. Synth. Catal.* **2018**, *360*, 1735; b) S. Karmakar, A. Silamkoti, N. A. Meanwell, A. Mathur, A. K. Gupta, *Adv. Synth. Catal.* **2021**, *363*, 3693; c) S. K. Parida, T. Mandal, S. Das, S. K. Hota, S. D. Sarkar, S. Murarka, *ACS Catal.* **2021**, *11*, 1640; d) J. E. Leffler, L. J. Story, *J. Am. Chem. Soc.* **1967**, *89*, 2333; e) J. I. Concepción, C. G. Francisco, R. Freire, R. Hernández, J. A. Salazar, E. Suárez, *J. Org. Chem.* **1986**, *51*, 402; f) J. Xie, P. Xu, H. Li, Q. Xue, H. Jin, Y. Cheng, C. Zhu, *Chem. Commun.* **2013**, *49*, 5672; g) Y. Liang, X. Zhang, D. W. C. MacMillan, *Nature* **2018**, *559*, 83; h) J.-L. Sui, X.-Q. Liu, S.-D. Li, P.-F. Huang, Y. Liu, J.-H. Li, *Chin. J. Chem.* **2024**, *42*, 3373.

[10] a) T. Patra, S. Mukherjee, J. Ma, F. Strieth-Kalthoff, F. Glorius, *Angew. Chem., Int. Ed.* **2019**, *58*, 10514; b) T. Patra, P. Bellotti, F. Strieth-Kalthoff, F. Glorius, *Angew. Chem., Int. Ed.* **2020**, *59*, 3172; c) G. Tan, M. Das, H. Keum, P. Bellotti, C. Daniliuc, F. Glorius, *Nat. Chem.* **2022**, *14*, 1174; d) G. Tan, F. Paulus, A. Rentería-Gómez, R. F. Lalisse, C. G. Daniliuc, O. Gutierrez, F. Glorius, *J. Am. Chem. Soc.* **2022**, *144*, 21664; e) G. Tan, F. Paulus, A. Petti, M.-A. Wiethoff, A. Lauer, C. Daniliuc, F. Glorius, *Chem. Sci.* **2023**, *14*, 2447.

[11] M. S. Crocker, J.-Y. Lin, R. Nsouli, N. D. McLaughlin, D. G. Musaev, A. Mehranfar, E. R. Lopez, L. K. G. Ackerman-Biegasiewicz, *Chem. Catal.* **2024**, *4*, 101131.

[12] S. Tamaki, T. Kusamoto, H. Tsurugi, *Chem. - Eur. J.* **2024**, *30*, e202402705.

[13] A. Fall, M. Magdei, M. Savchuk, S. Oudeyer, H. Beucher, J.-F. Brière, *Chem. Commun.* **2024**, *60*, 6316.

[14] S.-C. Kao, K.-J. Bian, X.-W. Chen, Y. Chen, A. A. Martí, J. G. West, *Chem. Catal.* **2023**, *3*, 100603.

[15] Y. Wang, L. Li, N. Fu, *ACS Catal.* **2022**, *12*, 10661.

[16] L. M. Denkler, M. A. Shekar, T. S. J. Ngan, L. Wylie, D. Abdullin, M. Engeser, G. Schnakenburg, T. Hett, F. H. Pilz, B. Kirchner, O. Schiemann, P. Kielb, A. Bunescu, *Angew. Chem., Int. Ed.* **2024**, *63*, e202403292.

[17] Y.-C. Lu, J. G. West, *Angew. Chem., Int. Ed.* **2023**, *62*, e202213055.

[18] N. Li, Y. Ning, X. Wu, J. Xie, W. Li, C. Zhu, *Chem. Sci.* **2021**, *12*, 5505.

[19] Z.-H. Wang, L. Wei, K.-J. Jiao, C. Ma, T.-S. Mei, *Chem. Commun.* **2022**, *58*, 8202.

[20] X. Lu, B. Xiao, L. Liu, Y. Fu, *Chem. - Eur. J.* **2016**, *22*, 11161.

[21] J. Xiao, Z. Li, J. Montgomery, *J. Am. Chem. Soc.* **2021**, *143*, 21234.

[22] J. Wang, S. Bai, C. Yang, X. Qi, *J. Am. Chem. Soc.* **2024**, *146*, 27070.

[23] K.-J. Bian, Y.-C. Lu, D. Nemoto, S.-C. Kao, X. Chen, J. G. West, *Nat. Chem.* **2023**, *15*, 1683.

[24] X.-K. Qi, L.-J. Yao, M.-J. Zheng, L. Zhao, C. Yang, L. Guo, W. Xia, *ACS Catal.* **2024**, *14*, 1300.

[25] S. Fernández-García, V. O. Chantzakou, F. Juliá-Hernández, *Angew. Chem., Int. Ed.* **2024**, *63*, e202311984.

[26] X. Jiang, Y. Lan, Y. Hao, K. Jiang, J. He, J. Zhu, S. Jia, J. Song, S.-J. Li, L. Niu, *Nat. Commun.* **2024**, *15*, 6115.

[27] B. M. Campbell, J. B. Gordon, E. R. Raguram, M. I. Gonzalez, K. G. Reynolds, M. Nava, D. G. Nocera, *Science* **2024**, *383*, 279.

[28] G. Shi, C. Shao, S. Pan, J. Yu, Y. Zhang, *Org. Lett.* **2015**, *17*, 38.

[29] J. Lin, Z. Li, J. Kan, S. Huang, W. Su, Y. Li, *Nat. Commun.* **2017**, *8*, 14353.

[30] W. Zhang, Z. Zou, Y. Wang, Y. Wang, Y. Liang, Z. Wu, Y. Zheng, Y. Pan, *Angew. Chem., Int. Ed.* **2019**, *58*, 624.

[31] M. Zhang, J. Chen, S. Huang, B. Xu, J. Lin, W. Su, *Chem Catal* **2022**, *2*, 1793.

[32] B. Yang, D. Yu, X.-H. Xu, F.-L. Qing, *ACS Catal.* **2018**, *8*, 2839.

[33] C. F. Meyer, S. M. Hell, A. Misale, A. A. Trabanco, V. Gouverneur, *Angew. Chem., Int. Ed.* **2019**, *58*, 8829.

[34] J. W. Beatty, J. J. Douglas, K. P. Cole, C. R. J. Stephenson, *Nat. Commun.* **2015**, *6*, 7919.

[35] D. Yin, D. Su, J. Jin, *Cell Rep. Phys. Sci.* **2020**, *1*, 100141.

[36] a) Q. Huang, C. Lou, L. Lv, Z. Li, *Chem. Commun.* **2024**, *60*, 12389; b) Y. Wu, X. Wang, Z. Wang, C. Chen, *Chem. Sci.* **2024**, *15*, 18497; c) Z. Song, L. Guo, C. Yang, W. Xia, *Org. Chem. Front.* **2024**, *11*, 4436; d) H. Guo, W. Lei, J. Ni, P. Xu, *Org. Lett.* **2024**, *26*, 9568; e) J. Liu, Z. Cui, J. Bi, X. He, Q. Ding, H. Zhu, C. Ma, *Front. Chem.* **2024**, *12*, 1481342.

[37] a) P. Xu, P. López-Rojas, T. Ritter, *J. Am. Chem. Soc.* **2021**, *143*, 5349; b) W. Su, P. Xu, T. Ritter, *Angew. Chem., Int. Ed.* **2021**, *60*, 24012; c) P. Xu, W. Su, T. Ritter, *Chem. Sci.* **2022**, *13*, 13611.

[38] Z. He, P. Dydio, *Angew. Chem., Int. Ed.* **2024**, *63*, e202410616.

[39] a) N. W. Dow, P. S. Pedersen, T. Q. Chen, D. C. Blakemore, A.-M. Dechert-Schmitt, T. Knauber, D. W. C. MacMillan, *J. Am. Chem. Soc.* **2022**, *144*, 6163; b) T. Q. Chen, P. S. Pedersen, N. W. Dow, R. Fayad, C. E. Hauke, M. C. Rosko, E. O. Danilov, D. C. Blakemore, A.-M. Dechert-Schmitt, T. Knauber, F. N. Castellano, D. W. C. MacMillan, *J. Am. Chem. Soc.* **2022**, *144*, 8296; c) P. S. Pedersen, D. C. Blakemore, G. M. Chinigo, T. Knauber, D. W. C. MacMillan, *J. Am. Chem. Soc.* **2023**, *145*, 21189.

[40] L. Candish, M. Freitag, T. Gensch, F. Glorius, *Chem. Sci.* **2017**, *8*, 3618.

[41] a) S. Kubosaki, H. Takeuchi, Y. Iwata, Y. Tanaka, K. Osaka, M. Yamawaki, T. Morita, Y. Yoshimi, *J. Org. Chem.* **2020**, *85*, 5362; b) Y. Tajimi, Y. Nachi, R. Inada, R. Hashimoto, M. Yamawaki, K. Ohkubo, T. Morita, Y. Yoshimi, *J. Org. Chem.* **2022**, *87*, 7405; c) R. Hashimoto, T. Furutani, H. Suzuki, Y. Yoshimi, *Synlett* **2024**, *35*, 357–361; d) K. Maeda, H. Saito, K. Osaka, K. Nishikawa, M. Sugie, T. Morita, I. Takahashi, Y. Yoshimi, *Tetrahedron* **2015**, *71*, 1117; e) K. Osaka, A. Usami, T. Iwasaki, M. Yamawaki, T. Morita, Y. Yoshimi, *J. Org. Chem.* **2019**, *84*, 9480; f) Y. Shinkawa, T. Furutani, T. Ikeda, M. Yamawaki, T. Morita, Y. Yoshimi, *J. Org. Chem.* **2022**, *87*, 11816; g) M. Yamawaki, K. Matsumoto, T. Furutani, S. Sugihara, Y. Yoshimi, *Polymer* **2024**, *308*, 127336; h) Y. Yoshimi, *Chem. Rec.* **2024**, *24*, e202300326.

[42] a) L. R. Malins, *Peptide Science* **2018**, *110*, e24049; b) P. Fang, W.-K. Pang, S. Xuan, W.-L. Chan, K. C.-F. Leung, *Chem. Soc. Rev.* **2024**, *53*, 11725.

[43] S. Bloom, C. Liu, D. K. Kölmel, J. X. Qiao, Y. Zhang, M. A. Poss, W. R. Ewing, D. W. C. MacMillan, *Nat. Chem.* **2018**, *10*, 205.

[44] a) T. Qin, J. Cornella, C. Li, L. R. Malins, J. T. Edwards, S. Kawamura, B. D. Maxwell, M. D. Eastgate, P. S. Baran, *Science* **2016**, *352*, 801; b) J. T. Edwards, R. R. Merchant, K. S. McClymont, K. W. Knouse, T. Qin, L. R. Malins, B. Vokits, S. A. Shaw, D.-H. Bao, F.-L. Wei, T. Zhou, M. D. Eastgate, P. S. Baran, *Nature* **2017**, *545*, 213; c) T. Qin, L. R. Malins, J. T. Edwards, R. R. Merchant, A. J. E. Novak, J. Z. Zhong, R. B. Mills, M. Yan, C. Yuan, M. D. Eastgate, P. S. Baran, *Angew. Chem., Int. Ed.* **2017**, *56*, 260; d) J. M. Smith, T. Qin, R. R. Merchant, J. T. Edwards, L. R. Malins, Z. Liu, G. Che, Z. Shen, S. A. Shaw, M. D. Eastgate, P. S. Baran, *Angew. Chem., Int. Ed.* **2017**, *56*, 11906; e) J. N. deGruyter, L. R. Malins, L. Wimmer, K. J. Clay, J. Lopez-Ogalla, T. Qin, J. Cornella, Z. Liu, G. Che, D. Bao, J. M. Stevens, J. X. Qiao, M. P. Allen, M. A. Poss, P. S. Baran, *Org. Lett.* **2017**, *19*, 6196.

Manuscript received: December 22, 2024

Revised manuscript received: February 28, 2025

Accepted manuscript online: March 3, 2025

Version of record online: ■■■